Position and momentum uncertainties of the normal and inverted harmonic oscillators under the minimal length uncertainty relation

Zachary Lewis* and Tatsu Takeuchi†

Department of Physics, Virginia Tech, Blacksburg, Virginia 24061, USA
(Received 13 September 2011; published 18 November 2011)

We analyze the position and momentum uncertainties of the energy eigenstates of the harmonic oscillator in the context of a deformed quantum mechanics, namely, that in which the commutator between the position and momentum operators is given by $[\hat{x}, \hat{p}] = i\hbar(1 + \beta\hat{p}^2)$. This deformed commutation relation leads to the minimal length uncertainty relation $\Delta x \geq (\hbar/2)(1/\Delta p + \beta\Delta p)$, which implies that $\Delta x \sim 1/\Delta p$ at small Δp while $\Delta x \sim \Delta p$ at large Δp. We find that the uncertainties of the energy eigenstates of the normal harmonic oscillator ($m > 0$), derived in L. N. Chang, D. Minic, N. Okamura, and T. Takeuchi, Phys. Rev. D **65**, 125027 (2002), only populate the $\Delta x \sim 1/\Delta p$ branch. The other branch, $\Delta x \sim \Delta p$, is found to be populated by the energy eigenstates of the "inverted" harmonic oscillator ($m < 0$). The Hilbert space in the inverted case admits an infinite ladder of positive energy eigenstates provided that $\Delta x_{\min} = \hbar\sqrt{\beta} > \sqrt{2}[\hbar^2/k|m|]^{1/4}$. Correspondence with the classical limit is also discussed.

I. INTRODUCTION

The consequences of deforming the canonical commutation relation between the position and momentum operators to

$$[\hat{x}, \hat{p}] = i\hbar(1 + \beta\hat{p}^2) \qquad (1)$$

have been studied in various contexts by many authors [1–9]. The main motivation behind this was to use such deformed quantum mechanical systems as models which obey the minimal length uncertainty relation (MLUR) [10]:

$$\Delta x \geq \frac{\hbar}{2}\left(\frac{1}{\Delta p} + \beta\Delta p\right). \qquad (2)$$

This relation is expected on fairly generic grounds in quantum gravity [11,12], and has been observed in perturbative string theory [13]. The MLUR implies the existence of a minimal length

$$\Delta x_{\min} = \hbar\sqrt{\beta}, \qquad (3)$$

below which the uncertainty in position, Δx, cannot be reduced. For quantum gravity, $\Delta x_{\min}$ would be the Planck scale, $\ell_P = \sqrt{\hbar G_N/c^3}$, while for string theory this would be the string length scale, $\ell_s = \sqrt{\alpha'}$. The investigation of said model systems could be expected to shed some light on the nature of these, and other, theories which possess a minimal length scale.

Note that the uncertainty in position which saturates the MLUR bound behaves as $\Delta x \sim 1/\Delta p$ for $\Delta p < 1/\sqrt{\beta}$, while $\Delta x \sim \Delta p$ for $1/\sqrt{\beta} < \Delta p$, as illustrated in Fig. 1. While we are familiar with the $\Delta x \sim 1/\Delta p$ behavior from

*zlewis@vt.edu
†takeuchi@vt.edu

canonical quantum mechanics, the $\Delta x \sim \Delta p$ behavior is quite novel. It behooves us to understand how it can come about, and how it can coexist with the canonical $\Delta x \sim 1/\Delta p$ behavior within a single quantum mechanical system. To this end, we calculate Δx and Δp for the energy eigenstates of the harmonic oscillator,

$$\hat{H} = \frac{1}{2}k\hat{x}^2 + \frac{1}{2m}\hat{p}^2, \qquad (4)$$

the wave functions of which were derived explicitly in Ref. [1]. We find that all of the eigenstates of this Hamiltonian inhabit the $\Delta x \sim 1/\Delta p$ branch, and not the other branch, as long as both the spring constant k and the mass m remain positive. The crossover happens when the inverse of the mass, $1/m$, is allowed to decrease through zero into the negative, in which case all the energy eigenstates will move smoothly over to the $\Delta x \sim \Delta p$
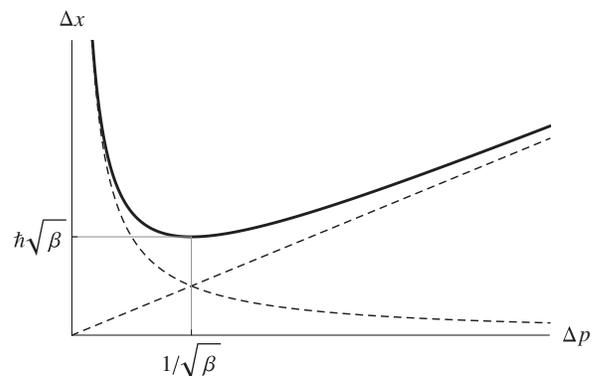

FIG. 1. The solid line indicates the lower bound on Δx as a function of Δp when they obey the minimal length uncertainty relation, Eq. (2). The dashed lines indicate $\Delta x = (\hbar/2)(1/\Delta p)$ and $\Delta x = (\hbar\beta/2)\Delta p$.

branch. The objective of this paper is to provide a detailed account of this result.

In the following, we solve the Schrödinger equation for the above Hamiltonian without assuming a specific sign for the mass m. The spring constant k is kept positive throughout. We find that the "inverted" harmonic oscillator with $k > 0$ and $m < 0$ admits an infinite ladder of normalizable positive energy eigenstates provided that

$$\Delta x_{\min} = \hbar\sqrt{\beta} > \sqrt{2}a, \tag{5}$$

where

$$a = \left[\frac{\hbar^2}{k|m|}\right]^{1/4} \tag{6}$$

is the characteristic length scale of the harmonic oscillator. The uncertainties Δx and Δp are calculated for the energy eigenstates, and the above mentioned crossover through $1/m = 0$ from the $\Delta x \sim 1/\Delta p$ branch to the $\Delta x \sim \Delta p$ branch is demonstrated.

We then take the classical limit of our deformed commutation relation and work out the evolution of the classical harmonic oscillator for both the positive- and negative-mass cases. It is found that for the inverted $m < 0$ case the time it takes for the particle to travel from $x = \pm\infty$ to the turning point and back is finite, demanding the compactification of x space, and also rendering the classical probability of finding the particle near the origin finite. This provides a classical explanation of why "bound" states are possible for the inverted harmonic oscillator in this modified mechanics.

II. QUANTUM STATES AND UNCERTAINTIES

A. Eigenvalues and eigenstates

The position and momentum operators obeying Eq. (1) can be represented in momentum space by [14]

$$\hat{x} = i\hbar(1 + \beta p^2)\frac{\partial}{\partial p}, \qquad \hat{p} = p. \tag{7}$$

The inner product between two states is

$$\langle\phi|\psi\rangle = \int_{-\infty}^{\infty} \frac{dp}{(1 + \beta p^2)} \phi^*(p)\psi(p). \tag{8}$$

This definition ensures the symmetricity of the operator $\hat{x}$. The Schrödinger equation for the harmonic oscillator in this representation is thus

$$\left[-\frac{\hbar^2 k}{2}\left\{(1 + \beta p^2)\frac{\partial}{\partial p}\right\}^2 + \frac{1}{2m}p^2\right]\Psi(p) = E\Psi(p). \tag{9}$$

Here, we do not assume $m > 0$ as usual, so the kinetic energy term can contribute with either sign. A change of variable from p to

$$\rho \equiv \frac{1}{\sqrt{\beta}}\arctan(\sqrt{\beta}p) \tag{10}$$

maps the region $-\infty < p < \infty$ to

$$-\frac{\pi}{2\sqrt{\beta}} < \rho < \frac{\pi}{2\sqrt{\beta}}, \tag{11}$$

and casts the $\hat{x}$ and $\hat{p}$ operators into the forms

$$\hat{x} = i\hbar\frac{\partial}{\partial\rho}, \qquad \hat{p} = \frac{1}{\sqrt{\beta}}\tan(\sqrt{\beta}\rho), \tag{12}$$

with inner product given by

$$\langle\phi|\psi\rangle = \int_{-\pi/2\sqrt{\beta}}^{\pi/2\sqrt{\beta}} d\rho\,\phi^*(\rho)\psi(\rho). \tag{13}$$

Note that $\hat{x}$ is the wave-number operator in ρ space, so the Fourier coefficients of the wave function in ρ space will provide the probability amplitudes for a discretized x space. Equation (9) is thus transformed into

$$\left[-\frac{\hbar^2 k}{2}\frac{\partial^2}{\partial\rho^2} + \frac{1}{2m\beta}\tan^2\sqrt{\beta}\rho\right]\Psi(\rho) = E\Psi(\rho). \tag{14}$$

In ρ space, the potential energy term $k\hat{x}^2/2$ effectively becomes the kinetic energy, and the kinetic energy term $\hat{p}^2/2m$ effectively becomes a tangent-squared potential which is inverted when $1/m < 0$. We next introduce dimensionless parameters and a dimensionless variable by

$$\kappa \equiv [\beta^2\hbar^2 k|m|]^{1/4} = \frac{\Delta x_{\min}}{a},$$

$$\varepsilon \equiv \frac{2|m|E\beta}{\kappa^2}, \tag{15}$$

$$\xi \equiv \frac{\sqrt{\beta}\rho}{\kappa},$$

where the length scale a was introduced in Eq. (6). The dimensionless variable ξ is in the range

$$-\frac{\pi}{2\kappa} < \xi < \frac{\pi}{2\kappa}, \tag{16}$$

and the inner product is

$$\langle\phi|\psi\rangle = \frac{\kappa}{\sqrt{\beta}}\int_{-\pi/2\kappa}^{\pi/2\kappa} d\xi\,\phi^*(\xi)\psi(\xi). \tag{17}$$

The dimension of the inner product has all been absorbed into the prefactor $1/\sqrt{\beta}$. The Schrödinger equation becomes

$$\left[\frac{\partial^2}{\partial\xi^2} \mp \frac{1}{\kappa^2}\tan^2\kappa\xi + \varepsilon\right]\Psi(\xi) = 0, \tag{18}$$

where the minus sign in front of the tangent-squared potential is for the case $m > 0$, and the plus sign for the case $m < 0$. Let $\Psi(\xi) = c^\lambda f(s)$, where $s \equiv \sin\kappa\xi$, $c \equiv \cos\kappa\xi = \sqrt{1 - s^2}$, and λ is a constant to be determined. The variable s is in the range

$$-1 < s < 1, \tag{19}$$

with inner product given by

$$\langle\phi|\psi\rangle = \frac{1}{\sqrt{\beta}}\int_{-1}^{1}\frac{ds}{c}\phi^*(s)\psi(s). \tag{20}$$

The equation for $f(s)$ is

$$(1-s^2)f'' - (2\lambda+1)sf'$$
$$+\left[\left\{\frac{\varepsilon}{\kappa^2}-\lambda\right\}+\left\{\lambda(\lambda-1)\mp\frac{1}{\kappa^4}\right\}\frac{s^2}{c^2}\right]f = 0. \tag{21}$$

We fix λ by requiring the coefficient of the tangent-squared term to vanish:

$$\lambda(\lambda-1)\mp\frac{1}{\kappa^4} = 0. \tag{22}$$

The solutions are

$$\lambda = \begin{cases} \frac{1}{2}+\sqrt{\frac{1}{4}+\frac{1}{\kappa^4}} \equiv \lambda_+ & (m>0), \\ \frac{1}{2}+\sqrt{\frac{1}{4}-\frac{1}{\kappa^4}} \equiv \lambda_- & (m<0), \end{cases} \tag{23}$$

where we have chosen the branches for which $\lambda \geq 1/2$ to prevent the inner product, Eq. (20), from blowing up at the domain boundaries. Note that $1 < \lambda_+$ while $\frac{1}{2} \leq \lambda_- < 1$, and that $\lambda_\pm \to 1$ in the limit $\kappa^2 = \beta\hbar\sqrt{k|m|} \to \infty$. The dependence of $\lambda_\pm$ on κ^2 is shown in Fig. 2. The λ_- branch does not extend below $\kappa^2 = 2$. Setting $\lambda = \lambda_+$ for $m > 0$, and $\lambda = \lambda_-$ for $m < 0$, simplifies Eq. (27) to

$$(1-s^2)f'' - (2\lambda+1)sf' + \left(\frac{\varepsilon}{\kappa^2}-\lambda\right)f = 0, \tag{24}$$

the sign of m being encoded in the value of λ. Since $f(s)$ should be nonsingular at $s = \pm 1$, we demand a polynomial solution to Eq. (24). This requirement imposes the following condition on the coefficient of f:

$$\frac{\varepsilon}{\kappa^2} - \lambda = n(n+2\lambda), \tag{25}$$

where n is a non-negative integer [15], and Eq. (24) becomes

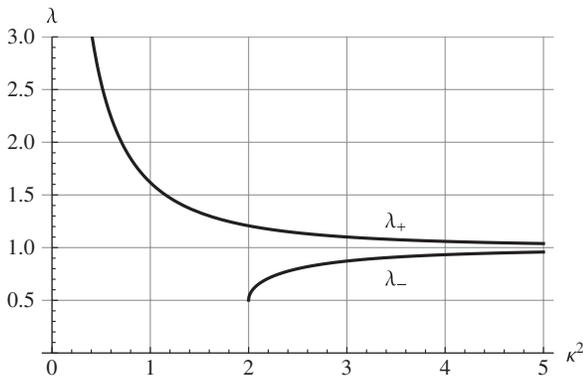$$(1-s^2)f'' - (2\lambda+1)sf' + n(n+2\lambda)f = 0. \tag{26}$$

FIG. 2.   Plots of λ_+ and λ_-, Eq. (23), as functions of $\kappa^2 = \beta\hbar\sqrt{k|m|}$.

The solution is the Gegenbauer polynomial

$$f(s) = C_n^\lambda(s), \tag{27}$$

which satisfies the following orthogonality relation:

$$\int_{-1}^{1} c^{2\lambda-1}C_n^\lambda(s)C_m^\lambda(s)ds = \frac{2\pi\Gamma(n+2\lambda)}{[2^\lambda\Gamma(\lambda)]^2 n!(n+\lambda)}\delta_{nm}. \tag{28}$$

The energy eigenvalues follow from the condition of Eq. (25). Replacing λ with $\lambda_\pm$, we obtain

$$\varepsilon_n^{(\pm)} = \kappa^2[n^2+(2n+1)\lambda_\pm] = \frac{n^2+(2n+1)\lambda_\pm}{\sqrt{\lambda_\pm|\lambda_\pm-1|}}$$
$$= \kappa^2\left(n^2+n+\frac{1}{2}\right)+(2n+1)\sqrt{\frac{\kappa^4}{4}\pm 1}, \tag{29}$$

or in the original dimensionful units,

$$E_n^{(\pm)} = \frac{1}{2\beta|m|}\frac{n^2+(2n+1)\lambda_\pm}{\lambda_\pm|\lambda_\pm-1|}$$
$$= \hbar\omega\left[\left(n+\frac{1}{2}\right)\sqrt{\frac{\beta^2m^2\hbar^2\omega^2}{4}\pm 1}\right.$$
$$\left.+\left(n^2+n+\frac{1}{2}\right)\frac{\beta|m|\hbar\omega}{2}\right]$$
$$= \frac{k}{2}\left[\left(n+\frac{1}{2}\right)\sqrt{(\Delta x_{\min})^4 \pm 4a^4}\right.$$
$$\left.+\left(n^2+n+\frac{1}{2}\right)(\Delta x_{\min})^2\right], \tag{30}$$

where $\omega = \sqrt{k/|m|}$. For the $m > 0$ case, we can take the limit $\Delta x_{\min} = \hbar\sqrt{\beta} \to 0$, and we recover

$$\lim_{\Delta x_{\min}\to 0} E_n^{(+)} = ka^2(n+\tfrac{1}{2}) = \hbar\omega(n+\tfrac{1}{2}). \tag{31}$$

For the $m < 0$ case, it is clear that we must have $\Delta x_{\min} \geq \sqrt{2}a$ for the square root in Eq. (30) to remain real. This is the condition we cited in Eq. (5). Therefore, the limit $\Delta x_{\min} = \hbar\sqrt{\beta} \to 0$ cannot be taken in this case for nonzero a. The two cases converge when $|m| \to \infty$, at which $a = 0$, and we find that the energy levels in that limit are

$$\lim_{|m|\to\infty} E_n^{(\pm)} = \frac{k}{2}(\Delta x_{\min})^2(n+1)^2. \tag{32}$$

Thus, the $1/m > 0$ and $1/m < 0$ cases connect smoothly at $1/m = 0$.

The normalized energy eigenfunctions are thus given by

$$\Psi_n^{(\lambda)}(p) = N_n^{(\lambda)}c^\lambda C_n^\lambda(s), \tag{33}$$

where

$$N_n^{(\lambda)} = \sqrt[4]{\beta}\left[2^\lambda \Gamma(\lambda)\sqrt{\frac{n!(n+\lambda)}{2\pi\Gamma(n+2\lambda)}}\right],$$

$$c = \cos\sqrt{\beta}\rho = \frac{1}{\sqrt{1+\beta p^2}}, \qquad (34)$$

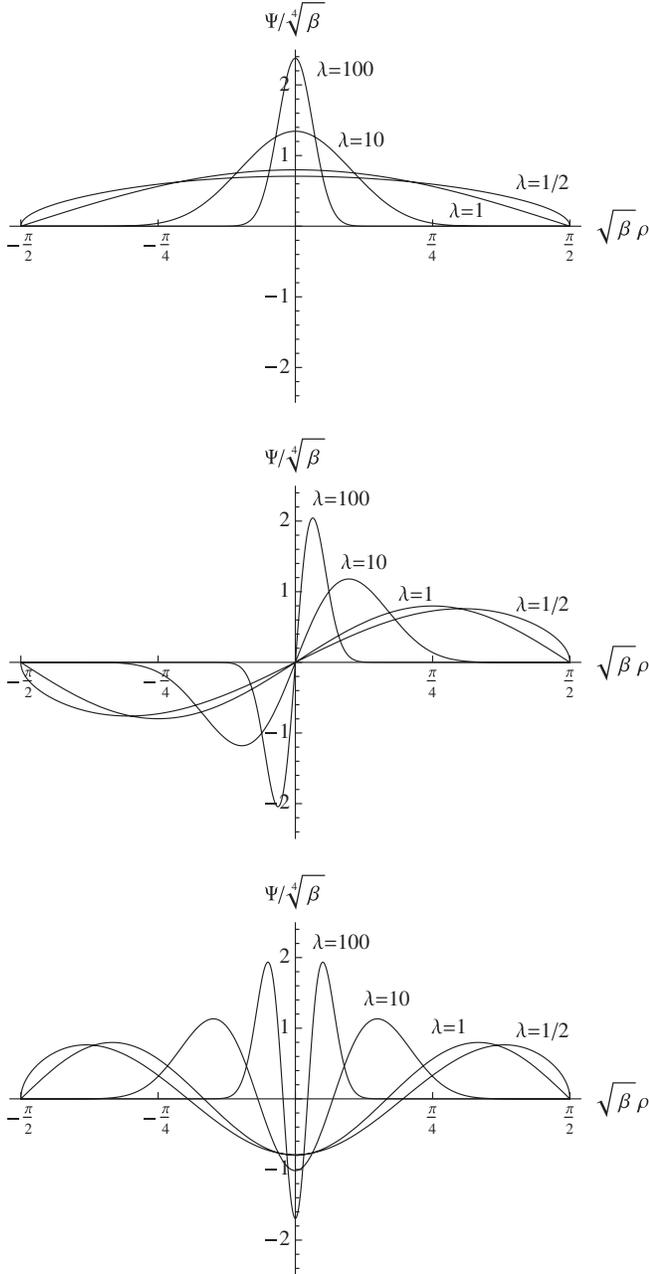$$s = \sin\sqrt{\beta}\rho = \frac{\sqrt{\beta}p}{\sqrt{1+\beta p^2}}.$$

The wave functions for the first few energy eigenstates for several representative values of λ are shown in Fig. 3.

B. Expectation values and uncertainties

Using the wave functions derived above, and the formula provided in the appendix, the expectation values of $\hat{x}$, $\hat{p}$, $\hat{x}^2$, and $\hat{p}^2$ for the energy eigenstates are found to be

$$\langle n, \lambda|\hat{x}|n, \lambda\rangle = 0,$$

$$\langle n, \lambda|\hat{p}|n, \lambda\rangle = 0,$$

$$\langle n, \lambda|\hat{x}^2|n, \lambda\rangle = (\hbar^2\beta)\frac{(\lambda+n)[(2\lambda-1)n+\lambda]}{(2\lambda-1)}, \qquad (35)$$

$$\langle n, \lambda|\hat{p}^2|n, \lambda\rangle = \frac{1}{\beta}\left(\frac{2n+1}{2\lambda-1}\right),$$

giving the uncertainties in $\langle\hat{x}\rangle$ and $\langle\hat{p}\rangle$ as

$$\Delta x_n = \Delta x_{\min}\sqrt{\frac{(\lambda+n)[(2\lambda-1)n+\lambda]}{(2\lambda-1)}},$$

$$\Delta p_n = \frac{1}{\sqrt{\beta}}\sqrt{\frac{2n+1}{2\lambda-1}}. \qquad (36)$$

For fixed n and fixed β, Δx_n is a monotonically decreasing function of λ in the range $\frac{1}{2} < \lambda < 1$, and a monotonically increasing one in the range $1 < \lambda$. Δp_n on the other hand is a monotonically decreasing function of λ throughout. Eliminating λ from the above expressions, we find

$$\frac{\Delta x_n}{\Delta x_{\min}} = \frac{1}{2\sqrt{\beta}\Delta p_n}\sqrt{[1+\beta\Delta p_n^2][(2n+1)^2+\beta\Delta p_n^2]}$$

$$\geq \frac{1}{2}\left(\frac{1}{\sqrt{\beta}\Delta p_n}+\sqrt{\beta}\Delta p_n\right), \qquad (37)$$

where the equality in the second line is saturated for the $n = 0$ case only. The first line gives the curve on the Δp-Δx plane that the point $(\Delta p_n, \Delta x_n)$ follows as λ is varied. Differentiating with respect to Δp_n we find

$$\frac{d}{d(\Delta p_n)}\left[\frac{\Delta x_n}{\Delta x_{\min}}\right]$$

$$= \frac{\beta^2\Delta p_n^4 - (2n+1)^2}{2\sqrt{\beta}\Delta p_n^2\sqrt{[1+\beta\Delta p_n^2][(2n+1)^2+\beta\Delta p_n^2]}}, \qquad (38)$$

indicating that the curve is flat at the $\lambda = 1$ point where $\Delta p_n = \sqrt{(2n+1)/\beta}$ and Δx_n reaches its minimum of $\Delta x_{\min}(n+1)$. Therefore, the $\lambda = 1$ point is the turn-around point where the uncertainties switch from the $\Delta x \sim 1/\Delta p$ behavior to the $\Delta x \sim \Delta p$ behavior. To go from one branch to another one must flip the sign of the mass m.

FIG. 3. λ-dependence of the wave functions of the first few energy eigenstates. The $\lambda > 1$ values correspond to $m > 0$, while the $\frac{1}{2} \leq \lambda < 1$ values correspond to $m < 0$. The $\lambda = 1$ case corresponds to the limit $|m| \to \infty$.
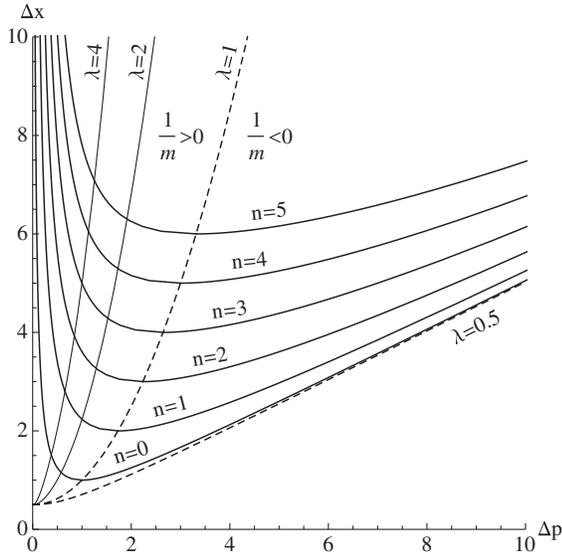
FIG. 4. Δp versus Δx for the lowest six energy eigenstates of the harmonic oscillator. Δx is in units of $\Delta x_{min} = \hbar\sqrt{\beta}$, while Δp is in units of $1/\sqrt{\beta} = \hbar/\Delta x_{min}$. The location of the state along the curves shown is determined by the value of λ defined in Eq. (23). The $\lambda = 1$ points correspond to the case $1/m = 0$. As $1/m$ is increased to the positive side, the value of λ will increase away from one and the state will move toward the left along the $\Delta x \sim 1/\Delta p$ branch. If $1/m$ is decreased into the negative, the value of λ will decrease toward $1/2$, and the state will move toward the right along the $\Delta x \sim \Delta p$ branch. The $n = 0$ curve corresponds to the minimal length uncertainty bound, Eq. (2).

Eliminating n from Eq. (36), we find

$$\frac{\Delta x_n}{\Delta x_{min}} = \frac{1}{2}\sqrt{(1 + \beta\Delta p_n^2)[1 + (2\lambda - 1)^2\beta\Delta p_n^2]}. \quad (39)$$

This gives the curve on which the points $(\Delta p_n, \Delta x_n)$ fall for constant λ. In particular, for $\lambda = 1$ this reduces to

$$\frac{\Delta x_n}{\Delta x_{min}} = \frac{1 + \beta\Delta p_n^2}{2}, \quad (40)$$

and gives the $1/m = 0$ boundary between the $1/m > 0$ and $1/m < 0$ regions in Δx-Δp space. These properties of the uncertainties have been plotted in Fig. 4.

C. Limiting cases

As shown in Fig. 4, the value of λ determines where the uncertainties $(\Delta p_n, \Delta x_n)$ are along their trajectories given by Eq. (37), with $\lambda > 1$ keeping the uncertainties on the $\Delta x \sim 1/\Delta p$ branch of the trajectory, while $\frac{1}{2} < \lambda < 1$ keeping them on the $\Delta x \sim \Delta p$ branch. Let us consider a few limiting values of λ to see the behavior of the solutions there.

1. $\lambda \rightarrow \infty$

The $\beta \rightarrow 0$ limit only exists for the $m > 0$ case where $\lambda = \lambda_+$. As $\beta \rightarrow 0$, the parameter λ_+ diverges to infinity as

$$\lambda = \lambda_+ \sim \frac{1}{m\hbar\omega\beta} \overset{\beta\rightarrow 0}{\rightarrow} \infty, \quad (41)$$

where $\omega = \sqrt{k/m}$. In that limit, the Gegenbauer polynomials become Hermite polynomials [15],

$$\lim_{\lambda\rightarrow\infty} n!\lambda^{-n/2}C_n^\lambda(x/\sqrt{\lambda}) = H_n(x), \quad (42)$$

and it is straightforward to show that

$$\lim_{\lambda\rightarrow\infty} \Psi_n^{(\lambda)}(p) = \frac{1}{\sqrt{2^n n!}}\frac{1}{\sqrt[4]{m\hbar\omega\pi}}\exp\left(-\frac{p^2}{2m\hbar\omega}\right)H_n\left(\frac{p}{\sqrt{m\hbar\omega}}\right), \quad (43)$$

which are just the canonical energy eigenstate wave functions in momentum space. The energy eigenvalues reduce to the usual ones given in Eq. (31). The uncertainties in this case are

$$\Delta x_n \overset{\lambda\rightarrow\infty}{\rightarrow} \sqrt{\frac{\hbar}{m\omega}\left(n + \frac{1}{2}\right)}, \qquad \Delta p_n \overset{\lambda\rightarrow\infty}{\rightarrow} \sqrt{\hbar m\omega\left(n + \frac{1}{2}\right)}, \quad (44)$$

which satisfy

$$\Delta x_n\Delta p_n \overset{\lambda\rightarrow\infty}{\rightarrow} \hbar\left(n + \frac{1}{2}\right) \geq \frac{\hbar}{2}. \quad (45)$$

2. $\lambda \rightarrow 1$

The limit $\lambda = 1$ is reached when β and k are kept constant while $|m|$ is taken to infinity. When $\lambda = 1$, the Gegenbauer polynomials become the Chebycheff polynomials of the second kind:

$$C_n^1(s) = U_n(s), \quad (46)$$

where

$$U_n(\cos\theta) = \frac{\sin(n + 1)\theta}{\sin\theta}. \quad (47)$$

Therefore,

$$\frac{\Psi_{2n}^{(1)}(p)}{\sqrt[4]{\beta}} = (-1)^n\sqrt{\frac{2}{\pi}}\cos[(2n + 1)\sqrt{\beta}\rho],$$

$$\frac{\Psi_{2n+1}^{(1)}(p)}{\sqrt[4]{\beta}} = (-1)^n\sqrt{\frac{2}{\pi}}\sin[(2n + 2)\sqrt{\beta}\rho]. \quad (48)$$

The energy eigenvalues in this limit were given in Eq. (32). Here, our procedure of keeping the spring constant k fixed while taking $|m|$ to infinity maintains the finiteness of E_n, while taking the kinetic energy contribution to E_n to zero. From the n-dependence of the energies, we can see that, in

this limit, the problem reduces to that of an infinite square well potential, of width $\pi/\sqrt{\beta}$, in ρ space. Indeed, the effective potential in ρ space was

$$\frac{1}{2m\beta}\tan^2(\sqrt{\beta}\rho)\overset{m\to\infty}{\to}\begin{cases}0 & \text{for } \rho\neq\pm\frac{\pi}{2\sqrt{\beta}},\\ \infty & \text{at } \rho=\pm\frac{\pi}{2\sqrt{\beta}}.\end{cases}\quad(49)$$

This can also be seen from the form of the energy eigenfunctions, which have reduced to simple sines and cosines. We will see in the next section that the classical solution also behaves as that of a particle in an infinite square well potential in ρ space in the same limit.

The uncertainties become

$$\Delta x_n\overset{\lambda\to1}{\to}\Delta x_{\min}(n+1),\qquad \Delta p_n\overset{\lambda\to1}{\to}\sqrt{\frac{(2n+1)}{\beta}},\quad(50)$$

as was shown in Fig. 4. Note that

$$\frac{\hbar}{2}\left[\frac{1}{\Delta p_n}+\beta\Delta p_n\right]=\Delta x_{\min}\frac{n+1}{\sqrt{2n+1}}$$
$$\leq\Delta x_{\min}(n+1)=\Delta x_n,\quad(51)$$

the bound being saturated only for the ground state $n=0$.

3. $\lambda\to\frac{1}{2}$

The $\lambda\to\frac{1}{2}$ limit is reached as $\Delta x_{\min}\to\sqrt{2}a$ when $m<0$. In this limit, the Gegenbauer polynomials become the Legendre polynomials, $C_n^{1/2}(s)=P_n(s)$, and we find

$$\frac{\Psi_n^{(1/2)}(p)}{\sqrt[4]{\beta}}=\sqrt{\frac{2n+1}{2}}\sqrt{c}P_n(s).\quad(52)$$

The integrals for $\langle\hat{x}^2\rangle$ and $\langle\hat{p}^2\rangle$ diverge in this limit, so both Δx_n and Δp_n are divergent for all n. However, the energy, which is the difference between $k\langle\hat{x}^2\rangle/2$ and $\langle\hat{p}^2\rangle/2|m|$, stays finite:

$$E_n^-=\frac{k}{2}(\Delta x_{\min})^2\left(n^2+n+\frac{1}{2}\right).\quad(53)$$

III. CLASSICAL STATES AND UNCERTAINTIES

As we have seen above, for values of β which maintain the inequality $\Delta x_{\min}=\hbar\sqrt{\beta}>\sqrt{2}a$, the harmonic oscillator Hamiltonian admits an infinite ladder of positive energy eigenstates even when $m<0$. Furthermore, these are states with finite Δx and Δp, implying that the particle is bound close to the phase space origin, just as in the $m>0$ case. But how can a particle be bound for an inverted harmonic oscillator? To gain insight into this question, we solve the corresponding classical equation of motion.

A. The classical equations of motion

We assume that the classical limit of our commutation relation, Eq. (1), is obtained by the usual correspondence between commutators and Poisson brackets:

$$\frac{1}{i\hbar}[\hat{A},\hat{B}]\to\{A,B\}.\quad(54)$$

That is, we assume

$$\{x,x\}=0,\qquad\{p,p\}=0,\qquad\{x,p\}=(1+\beta p^2).\quad(55)$$

Then, the equations of motion for the harmonic oscillator with Hamiltonian given by

$$H=\frac{1}{2}kx^2+\frac{1}{2m}p^2\quad(56)$$

are

$$\dot{x}=\{x,H\}=\frac{1}{m}(1+\beta p^2)p,$$
$$\dot{p}=\{p,H\}=-k(1+\beta p^2)x.\quad(57)$$

We allow m to take on either sign: if $m>0$, then $\dot{x}$ and p will have the same sign; if $m<0$ they will have opposite signs. Note that, even though the equations of motion of x and p have changed, the total energy will still be conserved. Consequently, the time evolution of x and p in phase space will be along the trajectory given by $H=$ constant. For the $m>0$ case this will be an ellipse, while for the $m<0$ case this will be a hyperbola.

To solve these equations, we change the variable p to ρ, which was introduced in Eq. (10) for the quantum case. Then, the equations become

$$\dot{x}=\frac{1}{m\sqrt{\beta}}\left[\frac{\tan(\sqrt{\beta}\rho)}{\cos^2(\sqrt{\beta}\rho)}\right]=\frac{1}{2m\beta}\frac{d}{d\rho}[\tan^2(\sqrt{\beta}\rho)],$$
$$\dot{\rho}=-kx.\quad(58)$$

Therefore,

$$\ddot{\rho}=-k\dot{x}=-\frac{k}{2m\beta}\frac{d}{d\rho}[\tan^2(\sqrt{\beta}\rho)],\quad(59)$$

which integrates to

$$\dot{\rho}^2=-\frac{k}{m\beta}[\tan^2(\sqrt{\beta}\rho)-C],\quad(60)$$

where C is the integration constant. Since we must have $\dot{\rho}^2>0$, the range of allowed values of C will depend on whether $m>0$ or $m<0$. We will consider the two cases separately.

B. $m>0$ case

When $m>0$, we introduce the angular frequency

$$\omega=\sqrt{\frac{k}{m}}\quad(61)$$

as usual. Then, Eq. (60) becomes

$$\sqrt{\beta}\dot{\rho} = \pm\omega\sqrt{C - \tan^2(\sqrt{\beta}\rho)}. \qquad (62)$$

In this case, we must have $C > 0$ for the content of the square root to be positive. Separating variables, we obtain

$$\frac{\sqrt{\beta}d\rho}{\sqrt{C - \tan^2(\sqrt{\beta}\rho)}} = \pm\omega dt, \qquad (63)$$

which integrates to

$$\sin(\sqrt{\beta}\rho(t)) = \sqrt{\frac{C}{1 + C}}\sin[\pm\sqrt{1 + C}\omega(t - t_0)], \quad (64)$$

where t_0 is the integration constant. Without loss of generality, we can choose the sign inside the square brackets to be plus. Setting the clock so that $t_0 = 0$, we obtain

$$\sqrt{\beta mk}x(t) = -\frac{\sqrt{\beta}}{\omega}\dot{\rho} = -\frac{\sqrt{C(1 + C)}\cos(\sqrt{1 + C}\omega t)}{\sqrt{1 + C\cos^2(\sqrt{1 + C}\omega t)}},$$

$$\sqrt{\beta}p(t) = \tan(\sqrt{\beta}\rho) = \frac{\sqrt{C}\sin(\sqrt{1 + C}\omega t)}{\sqrt{1 + C\cos^2(\sqrt{1 + C}\omega t)}},$$

$$(65)$$

and the energy is given by

$$E = \frac{k}{2}x(t)^2 + \frac{p(t)^2}{2m} = \frac{C}{2\beta m} > 0. \qquad (66)$$

The period of oscillation T is no longer equal to $2\pi/\omega$ when $\beta \neq 0$. It is now

$$T = \frac{2\pi}{\omega}\frac{1}{\sqrt{1 + C}}. \qquad (67)$$

Let

$$A \equiv \sqrt{\frac{C}{\beta mk}}. \qquad (68)$$

Then

$$E = \frac{1}{2}kA^2, \qquad (69)$$

and we can identify A as the oscillation amplitude in x. If we take the limit $\beta \to 0$ while keeping A fixed, we find

$$x(t)\overset{\beta \to 0}{\to} - A\cos(\omega t), \qquad p(t)\overset{\beta \to 0}{\to} Am\omega\sin(\omega t), \quad (70)$$

which shows that the canonical behavior is recovered in this limit. The behavior of the solution when $\beta \neq 0$ is compared with the $\beta = 0$ limit for several representative values of C in Fig. 5.

Another interesting limit is obtained by setting $C = 2mE\beta$ and letting $m \to \infty$ while keeping E and β fixed. In that limit,
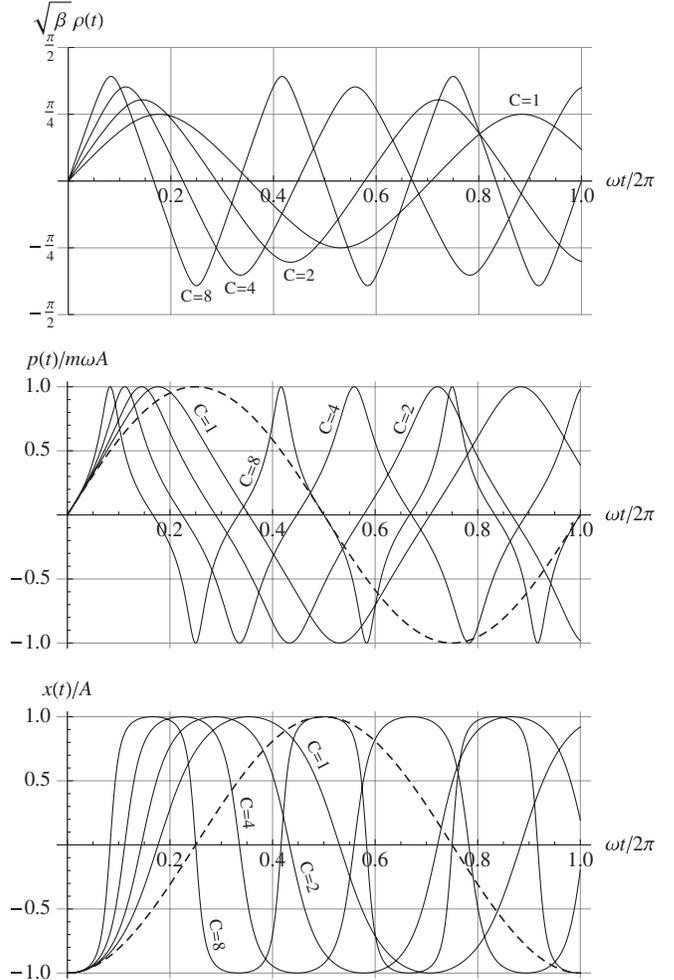

FIG. 5. The dependence of the classical behavior of a positive-mass particle in a harmonic oscillator potential on the parameter $C = 2mE\beta = \beta m^2\omega^2A^2$, where E is the particle's energy, and A is the amplitude of the oscillation in x. The dashed line indicates the undeformed $\beta = 0$ case, while the four solid lines indicate the $C = 1, 2, 4$, and 8 cases with larger values of C leading to shorter oscillation periods.

$$\sqrt{1 + C}\omega\overset{m \to \infty}{\to}\sqrt{2E\beta k} = \sqrt{\beta}kA \equiv \omega_0, \qquad (71)$$

and we find

$$\sqrt{\beta}\rho(t)\overset{m \to \infty}{\to}\arcsin[\sin(\omega_0 t)],$$

$$\sqrt{\beta}p(t)\overset{m \to \infty}{\to} + \frac{\sin(\omega_0 t)}{|\cos(\omega_0 t)|},$$

$$x(t)/A\overset{m \to \infty}{\to} - \frac{\cos(\omega_0 t)}{|\cos(\omega_0 t)|}.$$

$$(72)$$

The behavior of the solution in this limit is shown in Fig. 6. The motion of a particle in an infinite square well potential (in ρ space) is reproduced, in correspondence to the quantum $\lambda \to 1$ limit.
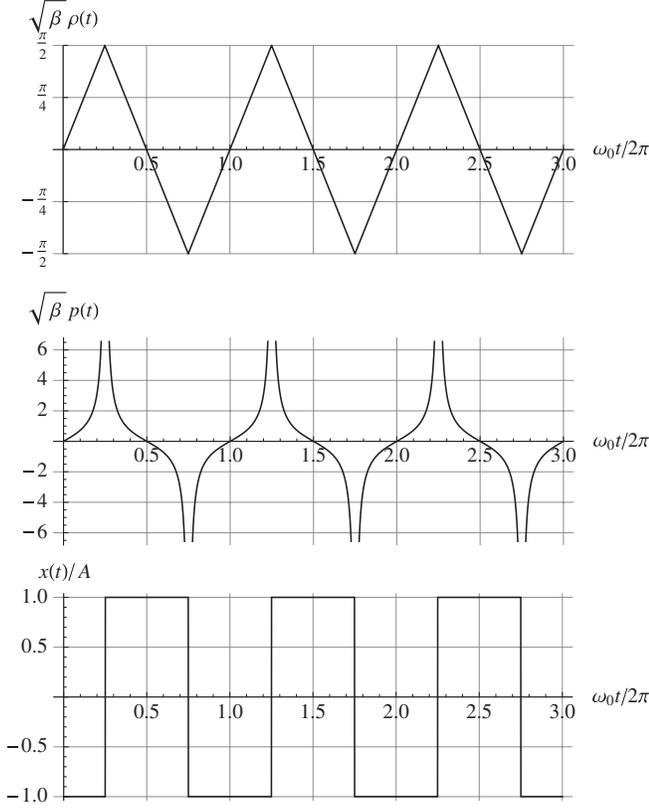
FIG. 6.   The classical behavior of a positive-mass particle in a harmonic oscillator potential with modified Poisson brackets, Eq. (55), in the limit $m \to \infty$ with $C = 2mE\beta$ where E and β are kept fixed. $\rho(t)$ and $x(t)$ take on the behavior of the position and momentum of a particle in an infinite square well.

C. $m < 0$ case

For the $m < 0$ case, by an abuse of notation, let us set

$$\omega = \sqrt{\frac{k}{|m|}}. \tag{73}$$

Then, Eq. (60) becomes

$$\sqrt{\beta}\dot{\rho} = \pm\omega\sqrt{\tan^2(\sqrt{\beta}\rho) - C}. \tag{74}$$

The integration constant C can have either sign in this case. We will consider the three cases $C < 0$, $C > 0$, and $C = 0$ separately.

1. $C < 0$ (positive energy) case

For the $C < 0$ case, let us write $C = -|C|$, and we have

$$\frac{\sqrt{\beta}d\rho}{\sqrt{\tan^2(\sqrt{\beta}\rho) + |C|}} = \pm\omega dt, \tag{75}$$

which integrates to

$$\sin(\sqrt{\beta}\rho(t))$$

$$= \begin{cases} \sqrt{\frac{|C|}{|C|-1}}\sin[\pm\sqrt{|C|-1}\omega(t-t_0)] & (|C| > 1) \\ \pm\omega(t-t_0) & (|C| = 1) \\ \sqrt{\frac{|C|}{1-|C|}}\sinh[\pm\sqrt{1-|C|}\omega(t-t_0)] & (|C| < 1), \end{cases} \tag{76}$$

where t_0 is the integration constant. We set $t_0 = 0$ in the following. From this, we find

$$\sqrt{\beta|m|k}x(t) = -\frac{\sqrt{\beta}}{\omega}\dot{\rho}$$

$$= \begin{cases} \mp\frac{\sqrt{|C|(|C|-1)}\cos(\pm\sqrt{|C|-1}\omega t)}{\sqrt{|C|\cos^2(\pm\sqrt{|C|-1}\omega t)-1}} & (|C| > 1) \\ \mp\frac{1}{\sqrt{1-(\omega t)^2}} & (|C| = 1) \\ \mp\frac{\sqrt{|C|(1-|C|)}\cosh(\pm\sqrt{1-|C|}\omega t)}{\sqrt{1-|C|\cosh^2(\pm\sqrt{1-|C|}\omega t)}} & (|C| < 1) \end{cases}$$

$$\sqrt{\beta}p(t) = \tan(\sqrt{\beta}\rho)$$

$$= \begin{cases} \frac{\sqrt{|C|}\sin(\pm\sqrt{|C|-1}\omega t)}{\sqrt{|C|\cos^2(\pm\sqrt{|C|-1}\omega t)-1}} & (|C| > 1) \\ \pm\frac{\omega t}{\sqrt{1-(\omega t)^2}} & (|C| = 1) \\ \frac{\sqrt{|C|}\sinh(\pm\sqrt{1-|C|}\omega t)}{\sqrt{1-|C|\cosh^2(\pm\sqrt{1-|C|}\omega t)}} & (|C| < 1). \end{cases} \tag{77}$$

In all three cases, we have

$$E = \frac{k}{2}x(t)^2 - \frac{p(t)^2}{2|m|} = \frac{|C|}{2\beta|m|} > 0. \tag{78}$$

Let

$$B \equiv \sqrt{\frac{|C|}{\beta|m|k}}. \tag{79}$$

Then

$$E = \tfrac{1}{2}kB^2, \tag{80}$$

and we can identify B as the distance of closest approach to the origin (aka impact parameter). Taking the limit $\beta \to 0$ while keeping B fixed, we find

$$x(t)\overset{\beta\to0}{\to}\mp B\cosh(\pm\omega t), \qquad p(t)\overset{\beta\to0}{\to}B|m|\omega\sinh(\pm\omega t), \tag{81}$$

which recovers the canonical solution. This behavior of $x(t)$ and $p(t)$ for the $\beta = 0$ case is compared with that for the $\beta \neq 0$ case for several representative values of C in Fig. 7.
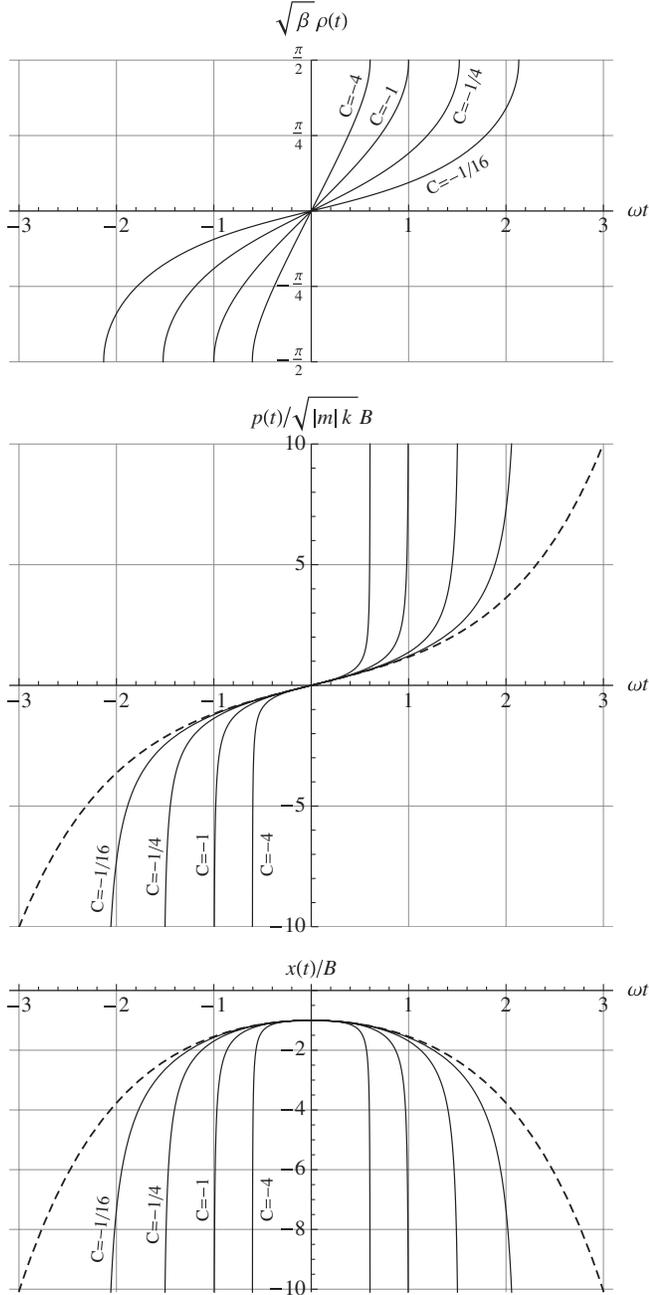
FIG. 7. The dependence of the classical behavior of a negative-mass particle in a harmonic oscillator potential on the parameter $C = -2\mu E\beta = -\beta|m|kB^2$, where E is the particle's energy, and B is the distance of closest approach to the origin in x space. Note that, due to the negative mass, $p(t)$ is negative when $\dot{x}(t)$ is positive, and vice versa. The dashed line indicates the undeformed $\beta = 0$ case. The four solid lines indicate the $C = -\frac{1}{16}$, $-\frac{1}{4}$, -1, and -4 cases, with larger values of $|C|$ leading to shorter travel times from $x = -\infty$ to $x = -B$ and back.

It should be noted that for any finite value of $C < 0$ it only takes a finite amount of time for the particle to travel from $(x, p) = (\pm\infty, \pm\infty)$ to $(x, p) = (\pm\infty, \mp\infty)$ or, equivalently, for $\sqrt{\beta}\rho$ to evolve from $\mp\pi/2$ to $\pm\pi/2$. We will

call this time $T/2$ for reasons that will become clear later. T is given by

$$T = \frac{4}{\omega} \times \begin{cases} \frac{1}{\sqrt{|C|-1}} \arccos\frac{1}{\sqrt{|C|}} & (|C| > 1) \\ 1 & (|C| = 1) \\ \frac{1}{\sqrt{1-|C|}} \operatorname{arccosh}\frac{1}{\sqrt{|C|}} & (|C| < 1). \end{cases}$$

(82)

This dependence on $C < 0$ is shown in Fig. 9.

2. $C > 0$ (negative energy) case

For the $C > 0$ case, we integrate

$$\frac{\sqrt{\beta}d\rho}{\sqrt{\tan^2(\sqrt{\beta}\rho) - C}} = \pm\omega dt \tag{83}$$

to obtain

$$\sin(\sqrt{\beta}\rho(t)) = \pm\sqrt{\frac{C}{1 + C}}\cosh[\pm\sqrt{1 + C}\omega(t - t_0)], \tag{84}$$

where t_0 is the integration constant, which we will set to zero in the following. The sign on the argument of the hyperbolic cosine is also irrelevant so we will set it to plus. From this, we find

$$\sqrt{\beta|m|k}x(t) = -\frac{\sqrt{\beta}}{\omega}\dot{\rho}$$
$$= \mp\frac{\sqrt{C(1 + C)}\sinh(\sqrt{1 + C}\omega t)}{\sqrt{1 - C\sinh^2(\sqrt{1 + C}\omega t)}},$$

$$\sqrt{\beta}p(t) = \tan(\sqrt{\beta}\rho)$$
$$= \pm\frac{\sqrt{C}\cosh(\sqrt{1 + C}\omega t)}{\sqrt{1 - C\sinh^2(\sqrt{1 + C}\omega t)}}, \tag{85}$$

and

$$E = \frac{k}{2}x(t)^2 - \frac{p(t)^2}{2|m|} = -\frac{C}{2\beta|m|} < 0. \tag{86}$$

Let

$$p_{\min} \equiv \sqrt{\frac{C}{\beta}}. \tag{87}$$

Then

$$E = -\frac{p_{\min}^2}{2|m|}, \tag{88}$$

and we can identify $p_{\min}$ as the magnitude of the momentum that the particle has at the origin $x = 0$. Taking the limit $\beta \to 0$ while keeping $p_{\min}$ constant, we find

$$\sqrt{\beta}\,\rho(t)$$

$$p(t)/p_{min}$$

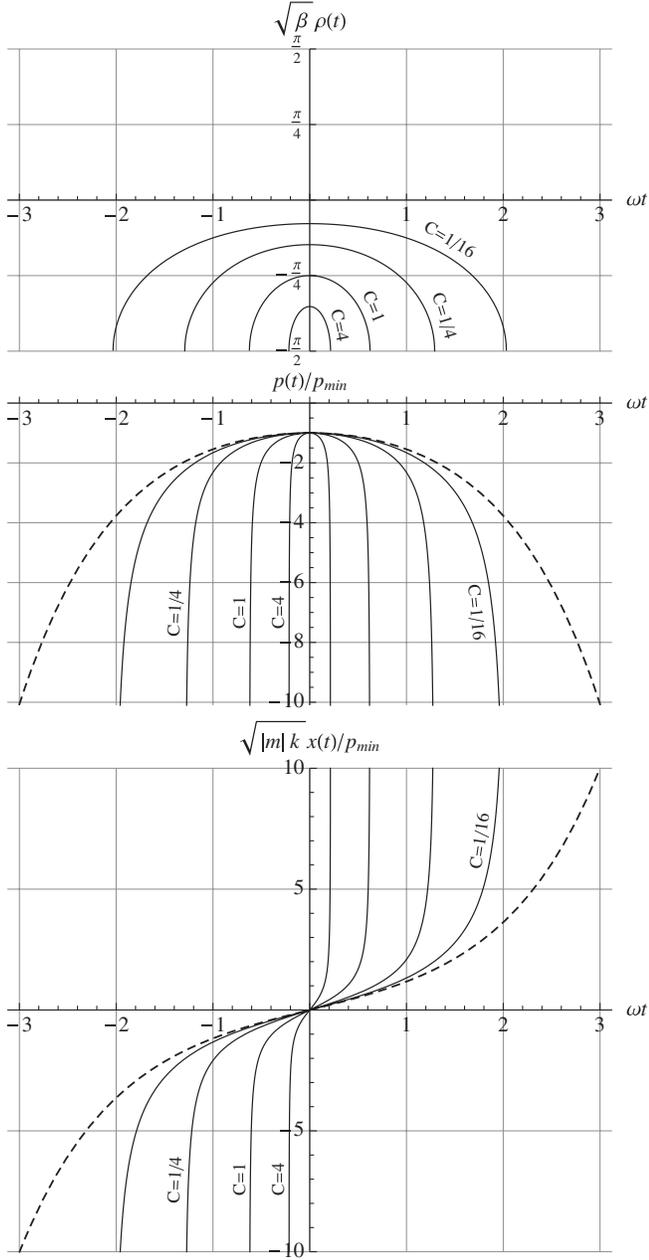$$\sqrt{|m|\,k}\,x(t)/p_{min}$$

FIG. 8. The dependence of the classical behavior of a negative-mass particle in a harmonic oscillator potential on the parameter $C = -2|m|E\beta = \beta p_{min}^2$, where E is the particle's energy, and p_{min} is the momentum of the particle at the origin $x = 0$. The dashed line indicates the undeformed $\beta = 0$ case. The four solid lines indicate the $C = +\frac{1}{16}, +\frac{1}{4}, +1$, and $C = +4$ cases with larger values of C leading to shorter travel times from $x = -\infty$ to $x = +\infty$.

$$x(t) \overset{\beta \to 0}{\longrightarrow} \mp \frac{p_{min}}{|m|\omega} \sinh(\pm\omega t),$$

$$p(t) \overset{\beta \to 0}{\longrightarrow} \pm p_{min} \cosh(\pm\omega t), \tag{89}$$

which recovers the canonical solution. This behavior of $x(t)$ and $p(t)$ for the $\beta = 0$ case is compared with that for
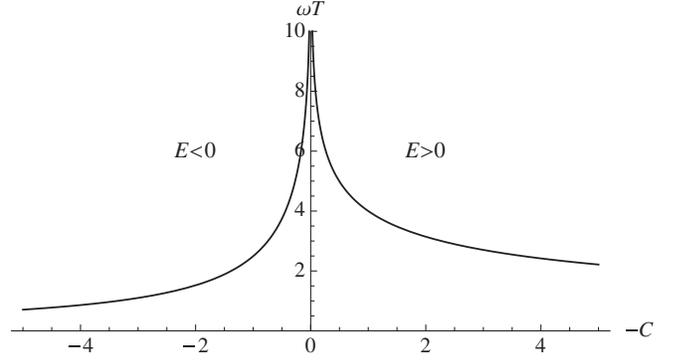

$$\omega T$$

FIG. 9. ωT as a function of $-C = 2|m|E\beta$, where $\omega = \sqrt{k/|m|}$, and E is the particle's energy. $T/2$ is the time it takes for the particle to traverse the entire trajectory.

the $\beta \neq 0$ case for several representative values of C in Fig. 8.

As in the $C < 0$ case, the time $T/2$ it takes for the particle to travel from $x = \mp\infty$ to $x = \pm\infty$ is finite when $\beta \neq 0$. T is given by

$$T = \frac{4}{\omega\sqrt{1+C}} \operatorname{arcsinh} \frac{1}{\sqrt{C}}. \tag{90}$$

This dependence on $C > 0$ is also shown in Fig. 9.

3. $C = 0$ (zero energy) case

For $C = 0$, Eq. (74) leads to

$$\frac{\sqrt{\beta}d\rho}{\tan(\sqrt{\beta}\rho)} = \pm\omega dt, \tag{91}$$

which integrates to yield

$$\sin(\sqrt{\beta}\rho) = \pm e^{\pm\omega(t-t_0)}, \tag{92}$$

with all combinations of signs allowed. Set the clock so that $t_0 = 0$. The solutions for the $t > 0$ region are

$$\sqrt{\beta|m|k}x(t) = -\frac{\sqrt{\beta}}{\omega}\dot{\rho} = \pm\frac{1}{\sqrt{e^{2\omega t}-1}},$$

$$\sqrt{\beta}p(t) = \tan(\sqrt{\beta}\rho) = \pm\frac{1}{\sqrt{e^{2\omega t}-1}}. \tag{93}$$

In this case, the particle starts out at $(x, p) = (\pm\infty, \pm\infty)$ and asymptotically approaches the origin, taking an infinite amount of time to get there.

D. Compactification

As we have seen, when $m < 0$ and $\beta \neq 0$, it only takes a finite amount of time for the particle to traverse the entire classical trajectory as long as the energy of the particle is nonzero. This means that we must specify what happens to the particle after it reaches infinity. For this, either we could compactify x space so that the particle which reaches $x = \pm\infty$ will return from $x = \mp\infty$, in which case the

momentum of the particle will bounce back from infinite walls at $p = \pm\infty$, or we could compactify p space so that the particle which reaches $p = \pm\infty$ will return from $p = \mp\infty$, in which case the position of the particle will bounce back from infinite walls at $x = \pm\infty$.

Here, we choose to compactify x space so that the $|m| \to \infty$ limit of the $m < 0$, $C < 0$ solution will match the $m \to \infty$ limit of the $m > 0$, $C > 0$ solution. This choice also agrees with the boundary condition we imposed in the quantum case, in which the wave function in ρ was demanded to vanish at the domain boundaries $\rho = \pm\pi/2\sqrt{\beta}$, which corresponds to placing infinite potential walls there. The $m > 0$, $C > 0$ solution was given by Eq. (72). Taking the $|m| \to \infty$ limit of Eq. (77) while keeping B fixed, we find
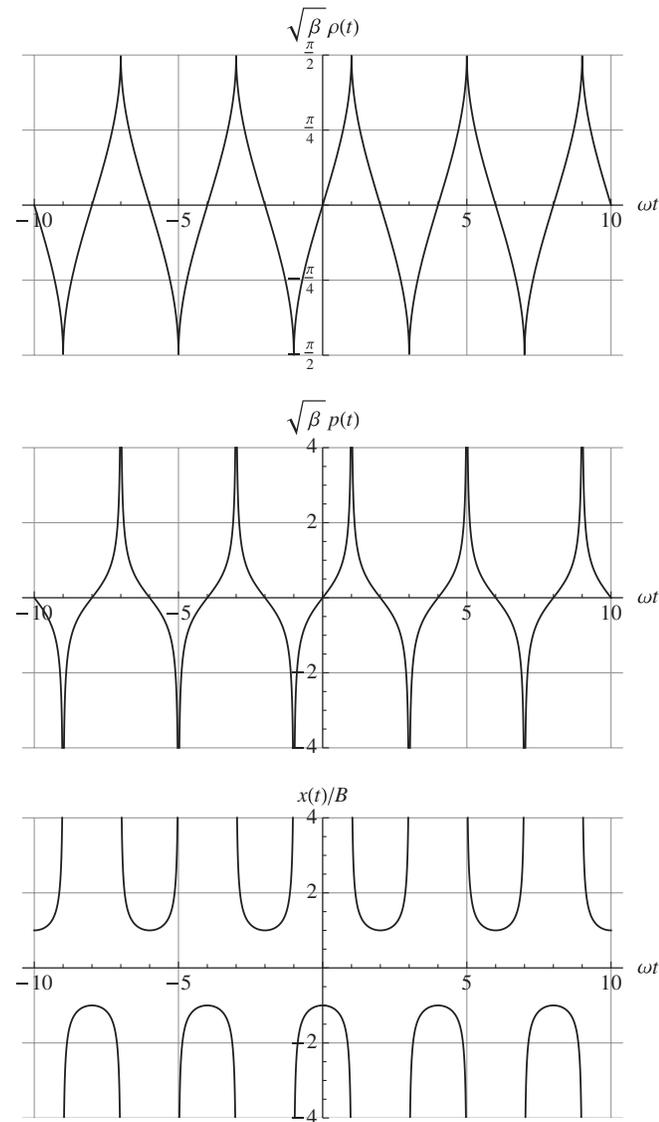

FIG. 10.   The periodic behavior of the negative-mass particle in a harmonic oscillator potential in compactified x space. The example shown is for $C = -1$.

$$\sqrt{|C| - 1}\,\omega \stackrel{m\to\infty}{\to} \sqrt{2E\beta k} = \sqrt{\beta}kB \equiv \omega_0, \qquad (94)$$

and

$$\sqrt{\beta}\rho(t) \stackrel{|m|\to\infty}{\to} \arcsin[\sin(\pm\omega_0 t)],$$
$$\sqrt{\beta}p(t) \stackrel{|m|\to\infty}{\to} +\frac{\sin(\pm\omega_0 t)}{|\cos(\pm\omega_0 t)|}, \qquad (95)$$
$$x(t)/B \stackrel{|m|\to\infty}{\to} \mp\frac{\cos(\pm\omega_0 t)}{|\cos(\pm\omega_0 t)|}.$$

which formally agrees with Eq. (72), and if graphed will lead to a figure similar to Fig. 6. The one significant difference is, however, that when the particle jumps from $x = \pm A$ to $x = \mp A$ in the $m > 0$ case it goes through $x = 0$, while when it jumps from $x = \pm B$ to $x = \mp B$ in the $m < 0$ case, it must go through $x = \infty$.

By compactifying x space, all motion when $E \neq 0$ will become periodic. For positive energy, the particle will oscillate through $x = \infty$, and the T calculated above becomes its oscillatory period. As an example, we plot the x-compactified solution for $C = -1$ in Fig. 10, for which the period is $T = 4/\omega$. Note that the period for the $m < 0$, $C < 0$ solution in the limit of $|m| \to \infty$ becomes

$$\lim_{|m|\to\infty} T = \lim_{|m|\to\infty} \frac{4}{\omega\sqrt{|C|^2 - 1}} \arccos\frac{1}{\sqrt{|C|}} = \frac{2\pi}{\omega_0}, \qquad (96)$$

the arccosine providing a $\pi/2$. For negative energy, the particle will repeatedly traverse the entire x space with period $T/2$.

E. Classical Probablities

Consider the $m < 0$, $C = -2|m|E\beta < 0$ case. $\sqrt{\beta}\rho$ evolves from $-\pi/2$ to $\pi/2$ in time $T/2$, that is,

$$\frac{T}{2} = \int_{-T/4}^{T/4} dt = \int_{-\pi/2\sqrt{\beta}}^{\pi/2\sqrt{\beta}} \frac{dt}{d\rho} d\rho = \int_{-\pi/2\sqrt{\beta}}^{\pi/2\sqrt{\beta}} \frac{d\rho}{\dot{\rho}}$$
$$= \frac{1}{\omega} \int_{-\pi/2\sqrt{\beta}}^{\pi/2\sqrt{\beta}} \frac{\sqrt{\beta}d\rho}{\sqrt{\tan^2(\sqrt{\beta}\rho) + |C|}}. \qquad (97)$$

Thus, we can identify

$$P(\rho) = \frac{2}{\omega T} \frac{\sqrt{\beta}}{\sqrt{\tan^2(\sqrt{\beta}\rho) + |C|}} \qquad (98)$$

as the classical probability density of the particle in ρ space. The classical probability densities in p and x spaces can be defined in a similar manner:
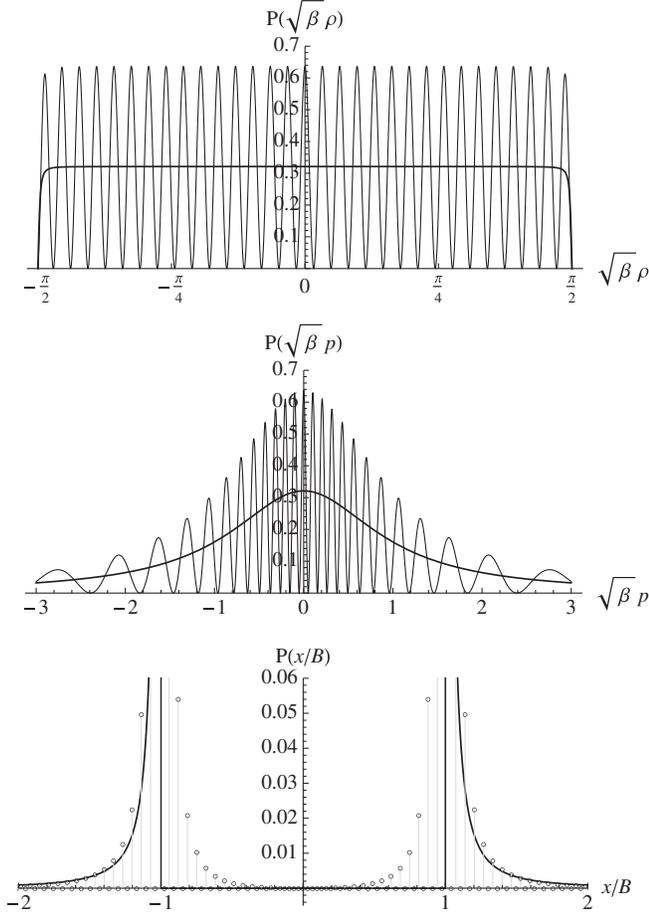
FIG. 11.   Comparison of quantum and classical probabilities in ρ, p, and x spaces for a negative-mass particle in a harmonic oscillator potential for the case $\lambda = \frac{3}{4}$ and $n = 30$, which corresponds to the classical $C = -2|m|E\beta = -5044$. The quantum distribution in x space is discrete due to the existence of the minimal length. There is also some seepage of the probability into classically forbidden regions in x space as is expected of quantum probabilities.

$$P(p) = P(\rho)\frac{d\rho}{dp} = \frac{2}{\omega T}\frac{\sqrt{\beta}}{(1 + \beta p^2)\sqrt{|C| + \beta p^2}},$$

$$P(x) = P(\rho)\frac{d\rho}{dx} = \frac{2}{\omega T}\frac{B^2}{\sqrt{x^2 - B^2}[|C|(x^2 - B^2) + B^2]}.$$

(99)

Comparing the energies of the quantum and classical solutions given in Eqs. (30) and (78), we can conclude that the correspondence is given by the relation

$$-C = \frac{n^2 + (2n + 1)\lambda}{\lambda(1 - \lambda)}, \qquad \frac{1}{2} < \lambda < 1.$$

(100)

We expect the quantum and classical probabilities to match for large n. As an example, we take $\lambda = \frac{3}{4}$ and $n = 30$, which correspond to

$$C = -5044, \qquad \kappa = \frac{2}{\sqrt[4]{3}},$$

$$B \overset{1 \ll n}{\approx} n \approx \Delta x_{\min} = 30\Delta x_{\min}.$$

(101)

The comparison of the quantum and classical probabilities for this case in ρ, p, and x spaces is shown in Fig. 11. If we average out the bumps in the quantum case, it is clear that the distributions agree, up to the typical quantum mechanical phenomenon of seepage of the probability into energetically forbidden regions. Thus, the existence of bound states with finite Δx and Δp in the quantum case can be associated with the fact that the particle spends a finite amount of time near the phase space origin in the classical limit.

IV. SUMMARY AND DISCUSSION

We have solved for the eigenstates of the harmonic oscillator Hamiltonian under the assumption of the deformed commutation relation between $\hat{x}$ and $\hat{p}$ as given in Eq. (1), with the objective of calculating their uncertainties in position and momentum.

For the normal harmonic oscillator with positive mass ($1/m > 0$), the eigenstates are found on the $\Delta x \sim 1/\Delta p$ branch of the MLUR, where decreasing $1/m$ leads to larger Δp, and thus smaller Δx. Somewhat surprisingly, $1/m$ can be decreased through zero into the negative, thereby "inverting" the harmonic oscillator, while still maintaining an infinite ladder of positive energy eigenstates so long as the condition $\Delta x_{\min}/\sqrt{2} > a \equiv [\hbar^2/k|m|]^{1/4}$ is satisfied. There, the eigenstates are found on the $\Delta x \sim \Delta p$ branch of the MLUR, where decreasing $1/m$ away from zero further into the negative leads to larger Δp, and thus larger Δx, with both diverging as a approaches the above bound from below. The $1/m = 0$ line separating the $\Delta x \sim 1/\Delta p$ and $\Delta x \sim \Delta p$ regions is given by Eq. (62).

Taking the classical limit by replacing our deformed commutator with a deformed Poisson bracket, we solve the corresponding classical equations of motion and find that the solutions for the inverted harmonic oscillator are such that the particle only takes a finite amount of time to traverse its entire trajectory. This leads to a finite classical probability density of finding the particle near the phase space origin, and provides an explanation of why bound states with discrete energy levels are possible in the quantum case.

One significant difference between the classical and quantum cases is, however, that the classical system has no restriction on the sign of the energy, whereas the quantum system only allows for positive energy eigenstates. The latter is guaranteed by the above mentioned condition on $\Delta x_{\min}$ and a. Indeed, the condition is equivalent to

$$E = \frac{k}{2}(\Delta x)^2 - \frac{1}{2|m|}(\Delta p)^2 > 0,$$

(102)

when one assumes $\Delta x \sim (\hbar\beta/2)\Delta p$.

We have found that the energy eigenstates of the harmonic oscillator only populate the $\Delta x \sim 1/\Delta p$ branch of the MLUR when the mass is positive, and only the $\Delta x \sim \Delta p$ branch when the mass is negative. A natural question to ask is whether some superposition of the energy eigenstates could cross over the $1/m = 0$ line to the other side. For the free particle, which can be considered the $k = 0$ limit of the harmonic oscillator, the answer is in the affirmative. In that case, the uncertainties of the energy eigenstates are $\Delta p = 0$ and $\Delta x = \infty$. Superpositions of these states, with uncertainties positioned anywhere along the MLUR bound, can be easily constructed, as will be discussed in detail in a subsequent paper [16]. Is a similar "crossover" possible for the $k \neq 0$ case?

Another interesting question is whether it is possible to construct classically behaving "coherent states" in either of these mass sectors, and whether their uncertainties are contained as they evolve in time. In particular, when the mass is negative, the classical equations of motion call for the particle to move at arbitrarily large speeds. What is the corresponding quantum phenomenon? We are also assuming that Eq. (1) embodies the nonrelativistic limit of some relativistic theory with a minimal length. From that perspective, the infinite speed that the negative-mass particle attains seems problematic. Would such states not exist in the relativistic theory, or would they metamorphose into imaginary mass tachyons? These and various other related questions will be addressed in future works.

ACKNOWLEDGMENTS

APPENDIX: AN INTEGRAL FORMULA FOR GEGENBAUER POLYNOMIALS

The following integral formula for Gegenbauer polynomials is necessary in calculating the expectation value of $\hat{p}^2$. For two non-negative integers m and n such that $m \leq n$, and $\lambda > \frac{1}{2}$, we have

$$\int_{-1}^{1} c^{2\lambda - 3} C_m^{\lambda}(s) C_n^{\lambda}(s) ds$$
$$= \begin{cases} \frac{4\pi\Gamma(m+2\lambda)}{(2\lambda-1)[2^{\lambda}\Gamma(\lambda)]^2 m!} & \text{if } n - m = \text{even,} \\ 0 & \text{if } n - m = \text{odd,} \end{cases} \quad \text{(A1)}$$

where $c = \sqrt{1 - s^2}$. We were unable to find this result in any of the standard tables of integrals [15] though MATHEMATICA seems to be aware of it. Here we present a proof.

We start from recursion relations which can be found in Ref. [15]. In Sec. 8.933 of Gradshteyn and Ryzhik, we have

$$(n + 2\lambda)C_n^{\lambda}(x) = 2\lambda[C_n^{\lambda+1}(x) - xC_{n-1}^{\lambda+1}(x)],$$
$$nC_n^{\lambda}(x) = 2\lambda[xC_{n-1}^{\lambda+1}(x) - C_{n-2}^{\lambda+1}(x)]. \quad \text{(A2)}$$

Eliminating $C_{n-1}^{\lambda+1}(x)$ and then shifting λ by one unit, we obtain

$$C_n^{\lambda}(x) - C_{n-2}^{\lambda}(x) = \left(\frac{n + \lambda - 1}{\lambda - 1}\right)C_n^{\lambda-1}(x), \quad \text{(A3)}$$

which is Eq. 22.7.23 of Abramowitz and Stegun. Iterating this relation, we deduce that

$$C_{2k}^{\lambda}(x) = C_0^{\lambda}(x) + \sum_{i=1}^{k}\left(\frac{2i + \lambda - 1}{\lambda - 1}\right)C_{2i}^{\lambda-1}(x),$$
$$C_{2k+1}^{\lambda}(x) = C_1^{\lambda}(x) + \sum_{i=1}^{k}\left(\frac{2i + \lambda}{\lambda - 1}\right)C_{2i+1}^{\lambda-1}(x). \quad \text{(A4)}$$

Since

$$C_0^{\lambda}(x) = 1 = C_0^{\lambda-1}(x),$$
$$C_1^{\lambda}(x) = 2\lambda x = \left(\frac{\lambda}{\lambda - 1}\right)C_1^{\lambda-1}(x), \quad \text{(A5)}$$

we can write

$$C_{2k}^{\lambda}(x) = \sum_{i=0}^{k}\left(\frac{2i + \lambda - 1}{\lambda - 1}\right)C_{2i}^{\lambda-1}(x),$$
$$C_{2k+1}^{\lambda}(x) = \sum_{i=0}^{k}\left(\frac{2i + \lambda}{\lambda - 1}\right)C_{2i+1}^{\lambda-1}(x). \quad \text{(A6)}$$

Thus, the even C_n^{λ}'s can be expressed as a sum of the even $C_n^{\lambda-1}$'s, and the odd C_n^{λ}'s as a sum of the odd $C_n^{\lambda-1}$'s. Invoking the orthogonality relation, Eq. (28), which is valid when $\lambda > -\frac{1}{2}$, it is clear that

$$\int_{-1}^{1} c^{2\lambda - 3} C_{2k}^{\lambda}(s) C_{2\ell+1}^{\lambda}(s) ds = 0 \quad \text{(A7)}$$

for $\lambda > \frac{1}{2}$. So for the integral of Eq. (A1) to be nonzero, m and n must be both even, or both odd. For two non-negative integers k and ℓ such that $k \leq \ell$, we find

$$\int_{-1}^{1} c^{2\lambda-3} C_{2k}^{\lambda}(s) C_{2\ell}^{\lambda}(s) ds = \sum_{i=0}^{k} \sum_{j=0}^{\ell} \left(\frac{2i + \lambda - 1}{\lambda - 1}\right) \left(\frac{2j + \lambda - 1}{\lambda - 1}\right) \int_{-1}^{1} c^{2\lambda-3} C_{2i}^{\lambda-1}(s) C_{2j}^{\lambda-1}(s) ds$$

$$= \sum_{i=0}^{k} \left(\frac{2i + \lambda - 1}{\lambda - 1}\right)^2 \frac{2\pi\Gamma(2i + 2\lambda - 2)}{(2i + \lambda - 1)[2^{\lambda-1}\Gamma(\lambda - 1)]^2 (2i)!}$$

$$= \frac{2\pi}{[2^{\lambda-1}\Gamma(\lambda)]^2} \sum_{i=0}^{k} \frac{(2i + \lambda - 1)\Gamma(2i + 2\lambda - 2)}{(2i)!},$$

$$\int_{-1}^{1} c^{2\lambda-3} C_{2k+1}^{\lambda}(s) C_{2\ell+1}^{\lambda}(s) ds = \sum_{i=0}^{k} \sum_{j=0}^{\ell} \left(\frac{2i + \lambda}{\lambda - 1}\right) \left(\frac{2j + \lambda}{\lambda - 1}\right) \int_{-1}^{1} c^{2\lambda-3} C_{2i+1}^{\lambda-1}(s) C_{2j+1}^{\lambda-1}(s) ds$$

$$= \sum_{i=0}^{k} \left(\frac{2i + \lambda}{\lambda - 1}\right)^2 \frac{2\pi\Gamma(2i + 2\lambda - 1)}{(2i + \lambda)[2^{\lambda-1}\Gamma(\lambda - 1)]^2 (2i + 1)!}$$

$$= \frac{2\pi}{[2^{\lambda-1}\Gamma(\lambda)]^2} \sum_{i=0}^{k} \frac{(2i + \lambda)\Gamma(2i + 2\lambda - 1)}{(2i + 1)!}. \tag{A8}$$

The sums in the above expressions are given by

$$\sum_{i=0}^{k} \frac{(2i + \lambda - 1)\Gamma(2i + 2\lambda - 2)}{(2i)!} = \frac{\Gamma(2k + 2\lambda)}{2(2\lambda - 1)(2k)!}, \qquad \sum_{i=0}^{k} \frac{(2i + \lambda)\Gamma(2i + 2\lambda - 1)}{(2i + 1)!} = \frac{\Gamma(2k + 2\lambda + 1)}{2(2\lambda - 1)(2k + 1)!}. \tag{A9}$$

These relations can be proved by induction in k. Putting everything together, we obtain Eq. (A1).

Using this formula, we find the matrix elements of the operator $\hat{p}^2$ to be

$$\langle m, \lambda | \hat{p}^2 | n, \lambda \rangle = \langle n, \lambda | \hat{p}^2 | m, \lambda \rangle = \begin{cases} \frac{1}{\beta} \left[-\delta_{mn} + \frac{2\sqrt{(\lambda+m)(\lambda+n)}}{2\lambda-1} \sqrt{\frac{n!\Gamma(2\lambda+m)}{m!\Gamma(2\lambda+n)}} \right] & \text{for } n - m = \text{even}, \, m \leq n, \\ 0 & \text{for } n - m = \text{odd}. \end{cases} \tag{A10}$$

In particular, the diagonal elements are given by

$$\langle n, \lambda | \hat{p}^2 | n, \lambda \rangle = \frac{1}{\beta}\left(\frac{2n + 1}{2\lambda - 1}\right). \tag{A11}$$

The expectation value of $\hat{x}^2$ is obtained from

$$\frac{k}{2}\langle \hat{x}^2 \rangle = \langle \hat{H} \rangle - \frac{\langle \hat{p}^2 \rangle}{2m}. \tag{A12}$$

[1] L. N. Chang, D. Minic, N. Okamura, and T. Takeuchi, Phys. Rev. D **65**, 125027 (2002).

[2] H. Hinrichsen and A. Kempf, J. Math. Phys. (N.Y.) **37**, 2121 (1996); A. Kempf, J. Math. Phys. (N.Y.) **38**, 1347 (1997); Phys. Rev. D **54**, 5174 (1996); J. Phys. A **30**, 2093 (1997); A. Kempf and G. Mangano, Phys. Rev. D **55**, 7909 (1997).

[3] F. Brau, J. Phys. A **32**, 7691 (1999); F. Brau and F. Buisseret, Phys. Rev. D **74**, 036002 (2006).

[4] L. N. Chang, D. Minic, N. Okamura, and T. Takeuchi, Phys. Rev. D **65**, 125028 (2002); S. Benczik, L. N. Chang, D. Minic, N. Okamura, S. Rayyan, and T. Takeuchi, Phys. Rev. D **66**, 026003 (2002); Phys. Rev. A **72**, 012104 (2005); S. Z. Benczik, Ph.D. thesis, Virginia Tech, 2007; L. N. Chang, D.

Minic, and T. Takeuchi, Mod. Phys. Lett. A **25**, 2947 (2010); L. N. Chang, Z. Lewis, D. Minic, and T. Takeuchi, Adv. High Energy Phys. **2011**, 493514 (2011).

[5] S. Hossenfelder, M. Bleicher, S. Hofmann, J. Ruppert, S. Scherer, and H. Stoecker, Phys. Lett. B **575**, 85 (2003); U. Harbach, S. Hossenfelder, M. Bleicher, and H. Stoecker, Phys. Lett. B **584**, 109 (2004); U. Harbach and S. Hossenfelder, Phys. Lett. B **632**, 379 (2006); S. Hossenfelder, Phys. Rev. D **70**, 105003 (2004); Classical Quantum Gravity **23**, 1815 (2006); Phys. Rev. D **73**, 105013 (2006).

[6] S. Das and E. C. Vagenas, Phys. Rev. Lett. **101**, 221301 (2008); Can. J. Phys. **87**, 233 (2009); Phys. Rev. Lett. **104**,

119002 (2010); A. F. Ali, S. Das, and E. C. Vagenas, Phys. Lett. B **678**, 497 (2009); S. Basilakos, S. Das, and E. C. Vagenas, J. Cosmol. Astropart. Phys. 09 (2010) 027; S. Das, E. C. Vagenas, and A. F. Ali, Phys. Lett. B **690**, 407 (2010); **692**, 342(E) (2010).

[7] B. Bagchi and A. Fring, Phys. Lett. A **373**, 4307 (2009); A. Fring, L. Gouba, and F. G. Scholtz, J. Phys. A **43**, 345401 (2010); A. Fring, L. Gouba, and B. Bagchi, J. Phys. A **43**, 425202 (2010).

[8] R. Banerjee and S. Ghosh, Phys. Lett. B **688**, 224 (2010).

[9] P. Pedram, Europhys. Lett. **89**, 50 008 (2010); Int. J. Mod. Phys. D **19**, 2003 (2010); K. Nozari and P. Pedram, Europhys. Lett. **92**, 50 013 (2010); P. Pedram, K. Nozari, and S. H. Taheri, J. High Energy Phys. 03 (2011) 093.

[10] D. Amati, M. Ciafaloni, and G. Veneziano, Phys. Lett. B **216**, 41 (1989); E. Witten, Phys. Today **49**, No. 4, 24 (1996).

[11] J. A. Wheeler, Ann. Phys. (N.Y.) **2**, 604 (1957).

[12] C. A. Mead, Phys. Rev. **135**, B849 (1964); , M. Maggiore, Phys. Lett. B **304**, 65 (1993); L. J. Garay, Int. J. Mod. Phys. A **10**, 145 (1995).

[13] D. J. Gross and P. F. Mende, Phys. Lett. B **197**, 129 (1987); Nucl. Phys. **B303**, 407 (1988); D. Amati, M. Ciafaloni, and G. Veneziano, Phys. Lett. B **197**, 81 (1987); Int. J. Mod. Phys. A **3**, 1615 (1988).

[14] A. Kempf, G. Mangano, and R. B. Mann, Phys. Rev. D **52**, 1108 (1995).

[15] I. S. Gradshteyn and I. M. Ryzhik, *Table of Integrals, Series and Products* (Academic Press, New York, 2007), 7th ed.; M. Abramowitz and I. A. Stegun, *Handbook of Mathematical Functions, with Formulas, Graphs, and Mathematical Tables* (Dover, New York, 1965).

[16] Z. Lewis and T. Takeuchi (unpublished).